FULL PAPER

BJC

British Journal of Cancer (2015) 112, 547–555 | doi: 10.1038/bjc.2014.637

Keywords: myxoid liposarcoma; tumour-associated macrophages; EGF receptor; heparin-binding EGF-like growth factor; PI3K/Akt

# Tumour-associated macrophages correlate with poor prognosis in myxoid liposarcoma and promote cell motility and invasion via the HB-EGF-EGFR-PI3K/Akt pathways

A Nabeshima[1], Y Matsumoto*[,1], J Fukushi[1], K Iura[2], T Matsunobu[1], M Endo[1], T Fujiwara[1], K Iida[1], Y Fujiwara[1], M Hatano[1], N Yokoyama[1], S Fukushima[1], Y Oda[2] and Y Iwamoto[1]

[1]*Department of Orthopaedic Surgery, Graduate School of Medical Sciences, Kyushu University, 3-1-1 Maidashi, Higashi-ku, 812-8582 Fukuoka, Japan and* [2]*Department of Anatomic Pathology, Graduate School of Medical Sciences, Kyushu University, 3-1-1 Maidashi, Higashi-ku, 812-8582 Fukuoka, Japan*

**Background:** Myxoid liposarcoma (MLS) is the second most common subtype of liposarcoma, and metastasis occurs in up to one-third of cases. However, the mechanisms of invasion and metastasis remain unclear. Tumour-associated macrophages (TAMs) have important roles in tumour invasion, metastasis, and/or poor prognosis. The aim of this study was to investigate the relationship between TAMs and MLS.

**Methods:** Using 78 primary MLS samples, the association between clinical prognosis and macrophage infiltration was evaluated by immunochemistry. The effects of macrophages on cell growth, cell motility, and invasion of MLS cell lines were investigated *in vitro*. In addition, clinicopathological factors were analysed to assess their prognostic implications in MLS.

**Results:** Higher levels of CD68-positive macrophages were associated with poorer overall survival in MLS samples. Macrophage-conditioned medium enhanced MLS cell motility and invasion by activating epidermal growth factor receptor (EGFR), with the key ligand suggested to be heparin-binding EGF-like growth factor (HB-EGF). The phosphoinositide 3-kinase/Akt pathway was mostly involved in HB-EGF-induced cell motility and invasion of MLS. The expression of phosphorylated EGFR in MLS clinical samples was associated with macrophage infiltration. In addition, more significant macrophage infiltration was associated with poor prognosis even in multivariate analysis.

**Conclusions:** Macrophage infiltration in MLS predicts poor prognosis, and the relationship between TAMs and MLS may be a new candidate for therapeutic targets of MLS.

Myxoid liposarcoma (MLS) is the second most common subtype of liposarcoma, comprising ~30% of all liposarcomas and about 10% of all adult soft tissue sarcomas (Antonescu and Ladanyi, 2013). The morphologic spectrum of tumours ranges from purely myxoid tumours to the more aggressive highly cellular round cell liposarcoma. Primary myxoid liposarcoma with more than a 5% round cell component is associated with a poor clinical prognosis (Antonescu *et al*, 2001; Oda *et al*, 2005). The most commonly affected regions tend to be the deep compartments of the extremities. Metastasis occurs in up to one-third of cases and is characterized by a propensity to spread to unusual extra-pulmonary locations (Haniball *et al*, 2011; Asano *et al*, 2012). However, the mechanism of tumour progression in MLS remains unclear. Therefore, it is important to elucidate the mechanism and to discover new prognostic factors and medical treatment targets.

*Correspondence: Dr Y Matsumoto; E-mail: ymatsu@ortho.med.kyushu-u.ac.jp

Revised 20 October 2014; accepted 1 December 2014; published online 6 January 2015

Recent reports have shown that tumour malignancy is dependent upon interactions in the tumour microenvironment between tumour cells and stromal cells such as immune cells, fibroblasts, and endothelial cells (Kamura *et al*, 2010; Pietras and Ostman, 2010). In particular, tumour-associated macrophages (TAMs) are stromal cells that are known to promote tumour invasion, metastasis, and angiogenesis in various tumours (Condeelis and Pollard, 2006; Qian and Pollard, 2010). Tumour-associated macrophages produce and secrete growth factors, cytokines, and other inflammatory mediators that may have important roles in cancer progression (Condeelis and Pollard, 2006; Baay *et al*, 2011). These tumour-promoting functions are consistent with clinical studies showing that high macrophage density in many human cancer types is associated with increased tumour angiogenesis and metastasis, and/or a poor prognosis.

In carcinomas, the majority of studies show that greater TAM infiltration is associated with poor prognosis, suggesting that TAMs may promote tumour progression (Leek *et al*, 1996; Komohara *et al*, 2013). With regard to sarcomas, we previously reported that TAM infiltration predicts poor prognosis in Ewing sarcoma (Fujiwara *et al*, 2011). Lee *et al* (2008) reported that an increased density of infiltrating macrophages was associated with poor outcomes in non-gynaecologic leiomyosarcomas. In contrast, Buddingh *et al*, (2011) showed that TAMs were associated with reduced frequency of metastasis and improvement in overall survival in. Thus, the role of TAMs in sarcomas differs depending on sarcoma subtypes, and there are few findings regarding their role in MLS. In this study, we investigated the role of TAMs in MLS.

## MATERIALS AND METHODS

**Cell lines.** The myxoid liposarcoma cell lines MLS1765 and MLS402-91 were kindly provided by Dr Aman (Department of Clinical Genetics, University Hospital, Lund, Sweden) (Aman *et al*, 1992). The murine macrophage RAW264.7 cell line was obtained from the European Collection of Cell Cultures (Salisbury, Wiltshire, England), and the human monocyte cell line U937 was obtained from the American Type Culture Collection (Manassas, VA, USA). Cells were cultured in RPMI-1640 (Invitrogen, Carlsbad, CA, USA) supplemented with 10% fetal bovine serum (HyClone Laboratories, Inc., Logan, UT, USA), 100 units per ml penicillin, and 100 $\mu g\,ml^{-1}$ streptomycin at 37 °C in an atmosphere of 5% $CO_2$. To induce U937 differentiation into macrophage-like cells, 10 $ng\,ml^{-1}$ phorbol 12-myristate 13-acetate (Sigma-Aldrich, St Louis, MO, USA) dissolved in dimethyl sulfoxide was added for 72 h, and lipopolysaccharide 1 $\mu g\,ml^{-1}$ was added for an additional 48 h. In all, $1 \times 10^6$ cells from each cell line were placed in 10-cm dishes. After cell adhesion, the medium was changed to 10 ml per well serum-free RPMI, and incubated for 24 h. The medium was collected and the cellular debris was pelleted by centrifuging. The undiluted supernatant was used as the conditioned medium (CM) of each cell line.

**Reagents.** Recombinant human HB-EGF and anti-HB-EGF antibodies were purchased from R&D Systems (Minneapolis, MN, USA). Gefitinib was purchased from Cayman Chemical (Ann Arbor, MI, USA). Anti-EGF receptor antibody (D38B1) and anti-phosphorylated EGF receptor (pEGFR) antibody (Tyr1068, D7A5) were purchased from Cell Signaling Technology (CST; Danvers, MA, USA). Anti-CD68 antibody was purchased from Dako (Glostrup, Denmark). Anti-CD163 antibody was purchased from Leica Biosystems (Newcastle, UK). PD98059, LY294002, and U-73122 were purchased from Calbiochem (San Diego, CA, USA).

**Clinical samples.** The study protocol was approved by the Institutional Review Board at Kyushu University. A total of 93 MLS cases that were diagnosed between 1981 and 2012 were retrieved from the archives of the Department of Anatomical Pathology, Graduate School of Medical Sciences, Kyushu University, Fukuoka, Japan. In each case, MLS was diagnosed on the basis of histological features. All patients had been treated by marginal or wide resection. Tissues were collected during primary tumour biopsy or surgical resection; those obtained after radiation or chemotherapy treatment were omitted. Of the 93 cases identified, 15 were excluded, 4 because of lack of availability of adequate tissue, and 11 because of lack of follow-up data. Thus, 78 patients were included in the present study. Clinical data were obtained by reviewing patient records, and survival data were collected during the winter of 2013. Each case was evaluated according to the American Joint Committee on Cancer (AJCC) grading system.

**Immunohistochemistry.** Whole-section samples were fixed in 10% neutral buffered formalin and embedded in paraffin, and the sections were deparaffinised in xylene and rehydrated in ethanol. Antigen was retrieved by microwave pretreatment with 10 mM citrate buffer (pH 6.0) for CD68 and CD163, and 1 mM EDTA buffer (pH 8.0) for pEGFR. After peroxidase blocking with hydrogen peroxide, the sections were incubated with the following primary antibodies: anti-CD68 (1 : 100, Dako) and anti-CD163 (1 : 100, Leica Biosystems) 1 h at room temperature and anti-pEGFR (1 : 200, CST) overnight at 4 °C. EnVision System HRP Labelled Polymer (Dako) was used as a secondary antibody. The reaction products were visualized with 3-3 diaminobenzidine tetrahydrochloride and counterstained with haematoxylin. Assessment of macrophage number was performed by counting CD68-positive cells and CD163-positive cells in 10 random high power field (HPF) profiles. Expression of pEGFR was evaluated and samples were classified as negative when there was either no staining or weak staining in the cytoplasm and/or nucleus compared with the stromal elements, and as positive when there was moderate to strong staining. Images were acquired using an AX70 microscope equipped with a DP72 camera (both from Olympus Corp., Tokyo, Japan).

**Double fluorescent immunohistochemistry.** To identify the co-expression of CD68 and CD163, double fluorescent immunohistochemical staining was performed in 10 different MLS clinical samples. Tissue samples were deparaffinised, rehydrated, and antigen was retrieved by microwave with 10 mM citrate buffer (pH 6.0). After blocking with normal goat serum for 1 h, the samples were incubated with anti-CD68 (mouse IgG) and anti-CD163 (rabbit IgG, Santa Cruz) for 2 h. The reactions were visualised using secondary fluorescently labelled antibodies including goat anti-mouse Alexa Fluor 488 and goat anti-rabbit Alexa Fluor 546 (both from Invitrogen Corp.), mounted in Vectashield mounting medium containing DAPI (Vector Laboratories, Burlingame, CA, USA), and imaged using BZ-X710 fluorescence microscopy (Keyence Corp., Osaka, Japan).

**Transwell migration assay.** A migration assay was performed using Transwell chambers (Corning Costar Corp., Cambridge, MA, USA) as described previously (Kamura *et al*, 2010). In brief, MLS cell lines or RAW264.7 cells ($1.0 \times 10^5$ per well) were suspended in 100 $\mu$l serum-free RPMI and seeded in the upper chambers. The lower chambers were placed in 600 $\mu$l serum-free RPMI containing CM or the indicated growth factors, antibodies. The indicated inhibitors were added to both upper and lower chambers. RAW264.7 cells were permitted to migrate for 6 h, and MLS cells migrated for 12 h. The cells that migrated to the lower side of the filter were fixed and stained using a Diff-Quik kit (Sysmex, Kobe, Japan), and counted by examining six fields per filter under a microscope.

**Wound-healing assay.** Wound-healing assays were performed as described previously (Kamura *et al*, 2010). Confluent cell monolayers in 35-mm dishes were wounded by scraping with a micropipette tip. The cells were washed and then cultured in serum-free RPMI containing CM or the noted reagents and inhibitors. The degree of wound closure was assessed by measuring the distance between the wound edges after 0 and 12 h.

**Invasion assay.** Invasion assays were performed using the Biocoat Matrigel invasion chamber (BD Biosciences, Bedford, MA, USA) as described previously (Harimaya *et al*, 2000). Myxoid liposarcoma cell lines ($1.0 \times 10^5$ per well) were suspended in 100 $\mu$l serum-free RPMI and seeded in the Matrigel-coated upper chambers. The lower chambers were placed in 600 $\mu$l serum-free RPMI containing CM or the indicated growth factors and antibodies. The indicated inhibitors were added to both upper and lower chambers. After 24-h incubation, the filters were fixed and the number of cells was determined as described for the transwell migration assay.

**Western blot analysis.** Myxoid liposarcoma cells were stimulated with macrophage-conditioned medium (M-CM: RAW-CM and U937-CM) or HB-EGF 20 ng ml$^{-1}$ for 5 min. To inhibit the stimulation, various concentrations of gefitinib and anti-HB-EGF antibody were added for 2 h before the stimulation. After stimulation, the cells were lysed using CelLytic (Sigma-Aldrich) with a protease and phosphatase inhibitor cocktail (Complete Mini, PhosSTOP; Roche Diagnostics, Mannheim, Germany). Western blot analysis was performed as described previously (Fujiwara-Okada *et al*, 2013; Iida *et al*, 2013) with the following primary antibodies: pEGFR (1 : 500), EGFR (1 : 1000), and $\beta$-actin (1 : 2000, Santa Cruz Biotechnology, Santa Cruz, CA, USA).

**RNA preparation and PCR.** Total RNA from MLS clinical samples and cell lines was extracted using the Rneasy Lipid Tissue Mini kit and Rneasy kit (Qiagen, Hilden, Germany), respectively. PCR was performed as described previously (Fujiwara *et al*, 2011). The primers are summarized in Supplementary Table S1.

**Phospho-receptor tyrosine kinase analysis.** Phosphorylated receptor tyrosine kinases (RTKs) of MLS cell lines after stimulation by M-CM were detected using the Human Phospho-RTK Array kit (R&D Systems) according to the manufacturer's instructions. Myxoid liposarcoma cells were stimulated with or without M-CM for 5 min. The cell lysate was added to a nitrocellulose membrane that contained 49 different anti-RTK antibodies printed in duplicates, and incubated overnight at 4 °C. After washing, the membrane was incubated with anti-phospho-Tyrosine-HRP for 2 h at room temperature, and immunoreactivity was detected using Chemi Reagent Mix.

**EGFR signalling analysis.** Phosphorylated downstream signalling modules of EGFR after stimulation by HB-EGF were detected using the PathScan EGFR Signaling Antibody Array kit (CST) according to the manufacturer's instructions. In brief, MLS cells were stimulated with or without HB-EGF (20 ng ml$^{-1}$) for 5 min. The cell lysate was arrayed on a nitrocellulose-coated glass slide which antibodies were spotted in duplicates, and incubated overnight at 4 °C. After washing, the glass slide was incubated with a detection antibody cocktail for 1 h and HRP-linked streptavidin for 30 min at room temperature, and immunoreactivity was then detected using Chemi Reagent Mix.

**Statistical analysis.** Survival curves were calculated using the Kaplan–Meier method, and the log-rank test was used for survival analysis. Fisher's exact test was used to compare categorized variables. The hazard ratios for risk factors for death were evaluated using the Cox proportional hazards regression model. The Student's *t*-test was used for two-group comparisons. $P < 0.05$ was considered as statistically significant. Data in graphs are given as mean ± s.d. All data analysis was performed using a statistical software package (JMP9, SAS Institute Inc., Cary, NC, USA).

## RESULTS

**Infiltrating macrophages into MLS associated with poor clinical outcome.** To investigate whether infiltrating macrophages were associated with clinical outcome in patients with MLS, anti-CD68 antibodies were used to quantify the number of macrophages in 78 primary MLS clinical samples (Figure 1A). Clinicopathological data are summarized in Supplementary Table S2. Kaplan–Meier survival analysis was performed to determine the prognostic significance of macrophages, and showed that greater macrophage infiltration ($\geqslant$100 CD68 cells/10 HPF) was associated with poorer overall survival ($P = 0.0002$, Figure 1B). Macrophages have a wide phenotypic diversity and can be classified into two activation phenotypes, M1 and M2 (Goerdt and Orfanos, 1999). Classically, M1 macrophages are pro-inflammatory and can exert cytotoxic activity. In contrast, M2 macrophages are anti-inflammatory and promote angiogenesis and tissue remodelling. Tumour-associated macrophages often exhibit features of M2 macrophages and produce a number of cytokines and growth factors that promote tumour progression. To evaluate the M2 phenotype in infiltrating macrophages, we performed immunostaining with antibodies against CD163, a marker of M2 macrophages (Figure 1A), as well as Kaplan–Meier survival analysis (Figure 1B). Co-expression of CD68 and CD163 was assessed by double fluorescent immunohistochemical staining (Figure 1C). Higher levels of CD163-positive macrophages were also associated with poorer overall survival ($P = 0.0213$, Figure 1B). On the basis of these results, we suggest that a high percentage of the TAMs in MLS are M2 macrophages, and we hypothesized that MLS might have the ability to recruit macrophages that have a role in the malignant transformation in MLS. To investigate the potential mechanisms underlying recruitment of macrophages to MLS, a Transwell migration assay was performed. Myxoid liposarcoma cell line-conditioned medium (MLS-CM) significantly promoted cell migration of RAW264.7 cells, a murine macrophage cell line (Figure 1D), suggesting that the factors that promote macrophage recruitment were contained in MLS-CM. Next, expression profiles of cytokines and chemokines secreted by MLS cells were examined using the Luminex multiplex assay system. Remarkably, CCL2, CCL5, CXCL8, and VEGF, which are known to stimulate monocyte chemotaxis (Carr *et al*, 1994; Matsumoto *et al*, 2002), were secreted in MLS-CM (Supplementary Figure S1). Therefore, these MLS-secreted cytokines and chemokines are likely to be critical factors in recruiting macrophages into the tumour microenvironment of MLS.

**Macrophages upregulated the motility and invasion of MLS cells by phosphorylation of EGFR.** To elucidate the role of TAMs in the development and progression of MLS, we first performed a cell proliferation assay to measure the effect of RAW264.7 and U937 macrophages on the growth of MLS cells. The presence of M-CM did not affect MLS cell growth (Supplementary Figure S2). Next, we investigated the effect of M-CM on motility of MLS cells via Transwell migration assay and wound-healing assay. M-CM significantly upregulated chemotaxis and chemokinesis of MLS cells (Figure 2A and B). We also found that M-CM significantly promoted MLS cell invasion (Figure 2C), an important result as cell motility is a critical factor in tumour cell invasion. One of the mechanisms known to upregulate cell motility is activation of the RTK pathway (Hubbard and Miller, 2007). We used a phospho-RTK antibody array to determine which RTKs were activated in M-CM-stimulated MLS cells. Of 49 MLS cell RTKs, only EGFR was phosphorylated by M-CM (Figure 2D), which was also confirmed by western blot (Figure 2E; Supplementary Figure S3).

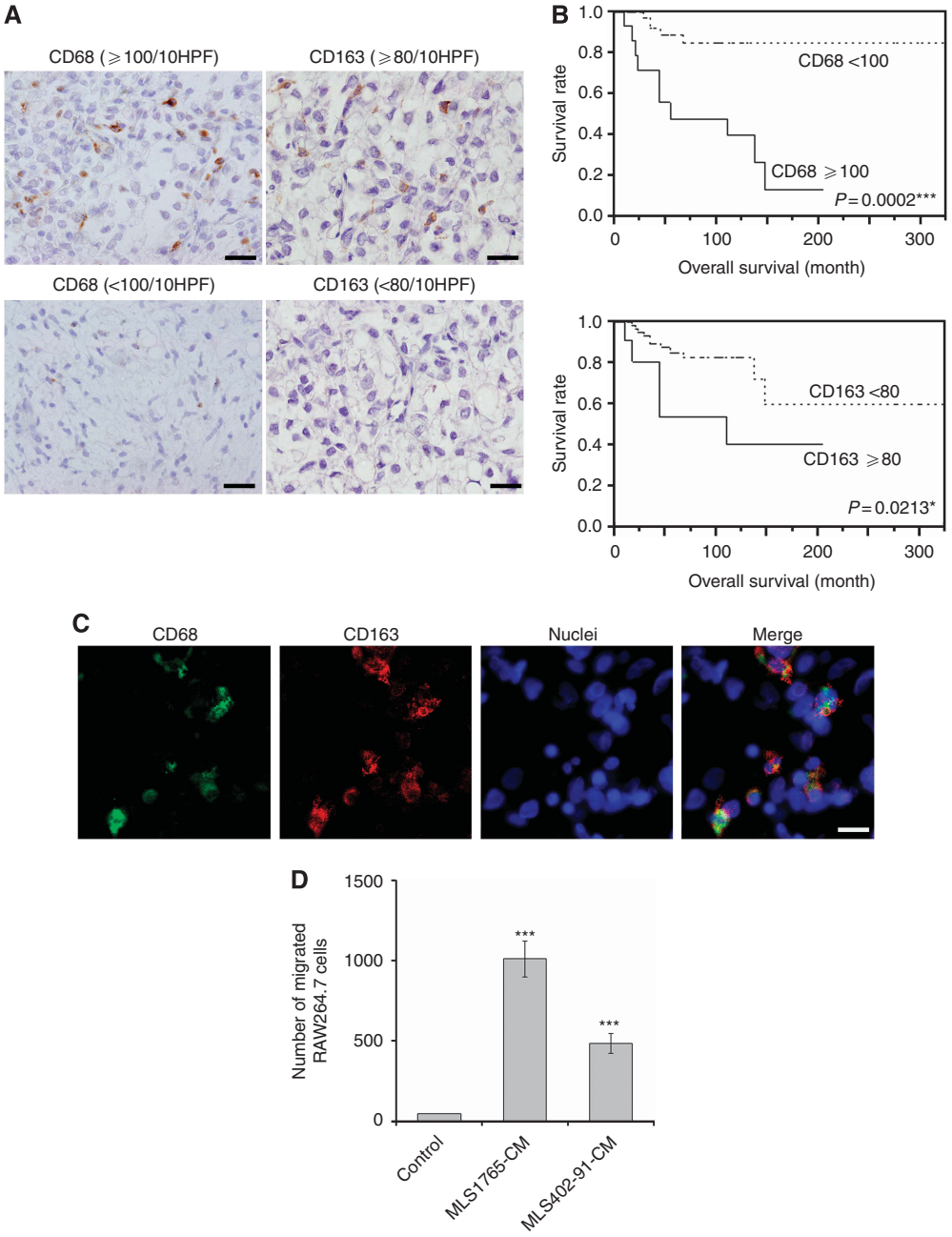


**Figure 1. Association between macrophage infiltration and poor prognosis in MLS.** (**A**) Immunohistochemical staining of human MLS sections using anti-CD68 and anti-CD163 antibodies. Upper panel shows cases with higher levels of macrophage infiltration (left, ⩾100 CD68 cells/10 HPF; right, ⩾80 CD163 cells/10 HPF), and lower panel demonstrates cases with lower levels of macrophage infiltration (left, <100 CD68 cells/10 HPF; right, <80 CD163 cells/10 HPF). Scale bars: 20 $\mu$m. (**B**) Kaplan–Meier survival curves for overall survival of all patients based on CD68-positive (upper) and CD163-positive (lower) macrophage infiltration. Log-rank test was performed to determine statistical significance, with $P<0.05$ defined as significant. (**C**) Co-expression of CD68 and CD163 in MLS clinical samples. Sections were immunostained for CD68 (green) and CD163 (red). Nuclei were visualized using DAPI (blue). Scale bar: 10 $\mu$m. (**D**) Migration of macrophages was examined using the Transwell system. The lower wells were filled with serum-free medium or medium conditioned by MLS1765 or MLS402-91, and RAW264.7 cell migration to the bottom surface of the Transwell was assessed. Results are presented as mean ± s.d. ***$P<0.001$ *vs* control.

Gefitinib, a tyrosine kinase inhibitor of EGFR, dose-dependently reduced M-CM-induced EGFR phosphorylation and also significantly suppressed MLS cell motility (Figure 2E and F; Supplementary Figure S3). These data suggested that activation of EGFR by macrophages could have a critical role in MLS motility. To investigate the correlation between macrophage infiltration and activation of EGFR in MLS, MLS clinical samples were immunostained with anti-pEGFR (Figure 2G and H). Twenty-seven cases (35%) were positive and fifty-one cases (65%) were negative. The results of immunostaining with anti-CD68 and anti-pEGFR clearly demonstrated that greater macrophage infiltration was significantly associated with positive pEGFR (odds ratio, 8.07; 95% confidence interval, 2.25–28.97; $P=0.0016$) (Figure 2I). In addition, greater macrophage infiltration was also significantly associated with metastasis (odds ratio, 16.85; 95% confidence interval, 4.02–70.57; $P=0.0001$) and higher AJCC stage (odds ratio, 6.67; 95% confidence interval, 1.68–26.39; $P=0.0072$) (Supplementary Table S3).

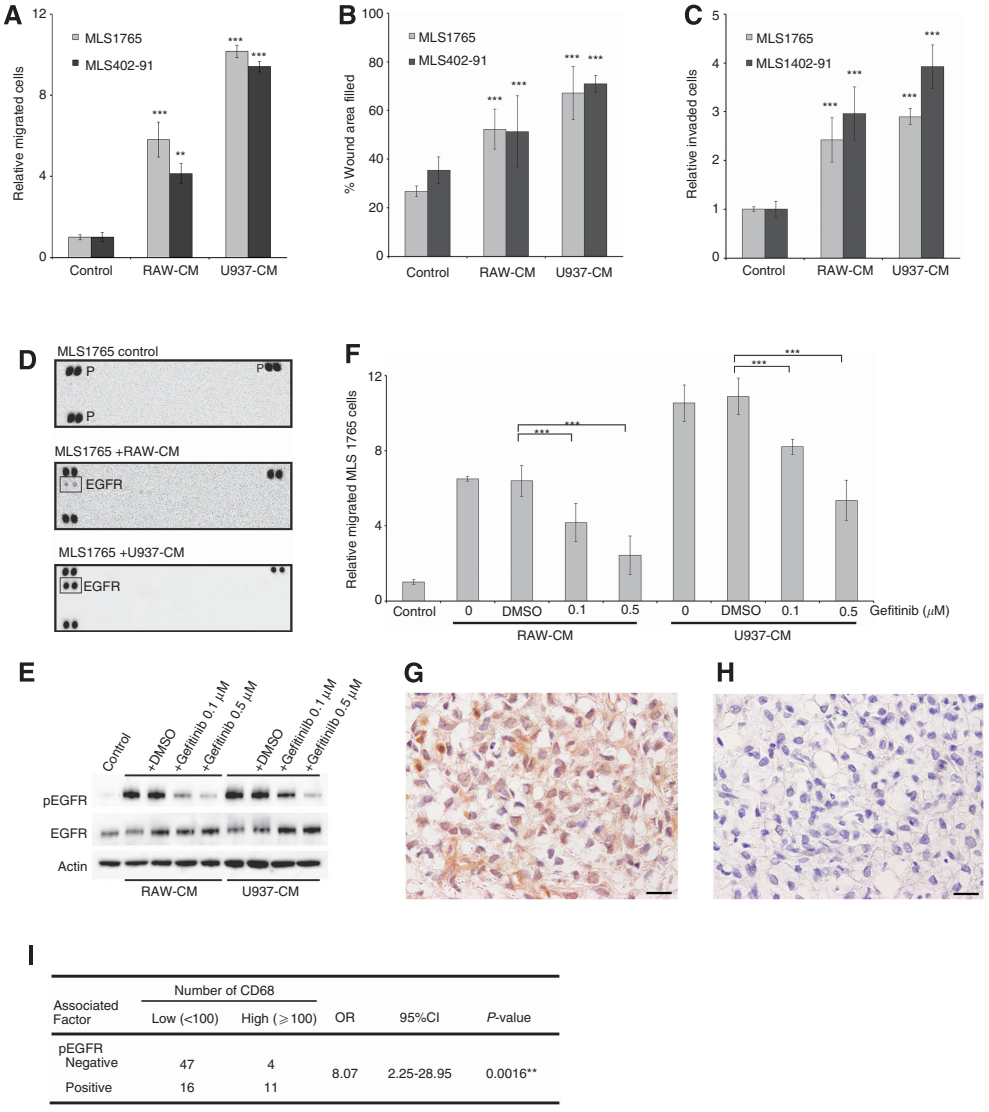


I

| Associated Factor | Number of CD68 | | OR | 95%CI | *P*-value |
|---|---|---|---|---|---|
| | Low (<100) | High (⩾100) | | | |
| pEGFR | | | | | |
| Negative | 47 | 4 | 8.07 | 2.25-28.95 | 0.0016** |
| Positive | 16 | 11 | | | |

Figure 2. Macrophages promoted the motility and invasion of MLS cells by phosphorylation of EGFR. (**A**) The chemotaxis of MLS1765 and MLS 402-91 cells was assessed by Transwell migration assay when the lower chambers were filled with serum-free medium, RAW-conditioned medium (CM), and U937-CM. Data are depicted as mean ± s.d. $^{**}P<0.01$, $^{***}P<0.001$ *vs* control. (**B**) Wound-healing assay was performed to assess the chemokinesis of MLS cells treated with RAW-CM and U937-CM. The percentage of wound closure corresponds to the distance between the wound edges. Data are shown as mean ± s.d. $^{***}P<0.001$ *vs* control. (**C**) Invasion of MLS cells in response to RAW-CM and U937-CM was assessed by invasion assay. Data are depicted as mean ± s.d. $^{***}P<0.001$ *vs* control. (**D**) Human Phospho-RTK Array Kit used to screen phosphorylated receptor tyrosine kinase of MLS1765 cells activated by RAW-CM and U937-CM. P, positive control. (**E**) Macrophage-CM-induced phosphorylation of EGFR in MLS1765 cells was assessed by western blot analysis with anti-EGFR and anti-pEGFR antibodies. MLS1765 cells were pre-treated with gefitinib (0.1 μM and 0.5 μM) for 2 h. Actin is shown as a loading control. (**F**) The effect of gefitinib on macrophage-CM-induced motility of MLS1765 cells was assessed by Transwell migration assay. Gefitinib (0.1 and 0.5 μM) was added to the upper and lower chambers. Data are shown as mean ± s.d. $^{***}P<0.001$. (**G**, **H**) Immunohistochemically stained human MLS sections using anti-pEGFR antibody. Positive staining for pEGFR (**G**), and negative (**H**). Scale bars: 20 μm. (**I**) Association between macrophage infiltration and expression of pEGFR in MLS clinical samples was analysed statistically. $^{**}P<0.01$ (Fisher's exact test); OR, odds ratio; CI, confidence interval.

**HB-EGF secreted by macrophages was a key ligand in activating EGFR of MLS cells.** Another important issue was identifying which EGFR ligands were dominant in M-CM-induced motility of MLS cells. The major ligands of EGFR are EGF, HB-EGF, transforming growth factor-α (TGFα), amphiregulin (AREG), epiregulin (EREG), epigen (EPGN), and betacellulin (BTC). Of these, HB-EGF and AREG were commonly expressed in RAW264.7 and U937 (Figure 3A). Importantly, HB-EGF significantly upregulated MLS cell motility (Figure 3B and C) and invasion (Figure 3D). In contrast, AREG did not promote MLS cell motility (Supplementary Figure S4). Anti-HB-EGF-neutralizing antibody inhibited the M-CM-induced motility of MLS cells and reduced their M-CM-induced EGFR phosphorylation (Figure 3E–G; Supplementary Figure S5). In contrast, anti-AREG neutralizing antibody had no effect on M-CM-induced cell motility (Supplementary Figure S4). Taken together, these results showed that macrophage-secreted HB-EGF was the key ligand in activating EGFR of MLS cells, and it strongly enhanced MLS cell motility and invasion. In addition, the expression of EGFR ligands in MLS clinical samples was evaluated by RT-PCR (Figure 3H). Among 10 MLS clinical samples, HB-EGF was the most commonly expressed ligand (90%), suggesting a clinical role of HB-EGF in the progression of MLS.

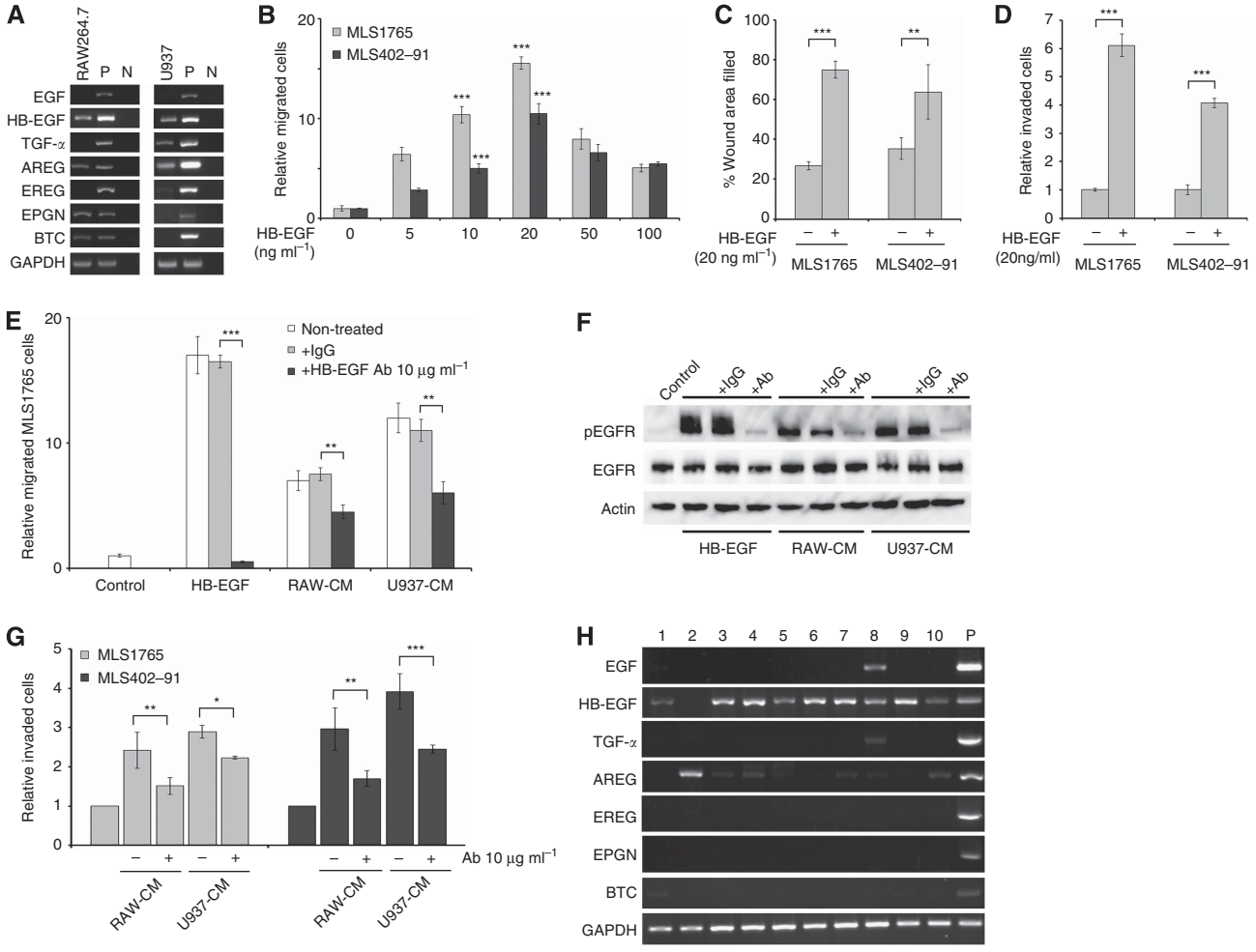


Figure 3. HB-EGF secreted by macrophages was the key ligand in activating EGFR of MLS cells. (**A**) The expression profiles of EGFR ligands in RAW264.7 and U937 cells were detected by RT-PCR. GAPDH was used as an internal control. P, positive control; N, negative control. (**B**) The chemotaxis of MLS1765 and MLS402-91 cells was assessed by Transwell migration assay with various concentrations of HB-EGF added to the lower chamber. Data are depicted as mean ± s.d. ***$P<0.001$ *vs* HB-EGF 0 ng ml$^{-1}$. (**C**) Wound-healing assay was performed to assess the chemokinesis of MLS cells treated with HB-EGF (20 ng ml$^{-1}$) for 12 h. Data are shown as mean ± s.d. **$P<0.01$, ***$P<0.001$. (**D**) Invasion of MLS cells in response to HB-EGF (20 ng ml$^{-1}$) was assessed by invasion assay. Data are depicted as mean ± s.d. ***$P<0.001$. (**E**) The effect of anti-HB-EGF–neutralizing antibody on macrophage-CM-induced motility of MLS1765 cells was assessed by Transwell migration assay. Anti-HB-EGF antibody (10 $\mu$g ml$^{-1}$) or normal IgG was added to lower chamber. Data are shown as mean ± s.d. **$P<0.01$, ***$P<0.001$. (**F**) The effect of anti-HB-EGF-neutralizing antibody on macrophage-CM-induced phosphorylation of EGFR in MLS1765 cells was assessed by western blot analysis with anti-EGFR and anti-pEGFR antibodies. Actin was used as a loading control. (**G**) Invasion assay was performed to assess the effect of anti-HB-EGF-neutralizing antibody on macrophage-CM-induced invasion. Data are depicted as mean ± s.d. *$P<0.05$, **$P<0.01$, ***$P<0.001$. (**H**) The expression profiles of EGFR ligands from 10 MLS clinical samples were detected by RT-PCR. GAPDH was used as an internal control. P, positive control.

**The PI3K/Akt pathway was the key downstream signalling pathway in HB-EGF-induced motility of MLS cells.** Activated EGFR stimulates a wide range of signalling modules, including PI3K/Akt, mitogen-activated protein kinase (MAPK) cascade, phospholipase C (PLC) $\gamma$, and signal transducer and activator of transcription 3 (STAT3). The PathScan EGFR Signalling Antibody Array was used to accurately detect the activated EGFR-stimulated downstream signalling modules in HB-EGF-induced MLS cells. HB-EGF stimulated EGFR, MEK1/2, Erk1/2, Akt, and PLC$\gamma$ (Figure 4A). STAT3 was not phosphorylated by HB-EGF stimulation. To identify the dominant downstream EGFR signalling pathway required for HB-EGF-induced cell motility, we used various pharmacological inhibitors, including LY294002 for PI3K/Akt, PD98059 for MEK and Erk, and U-73122 for PLC$\gamma$. LY294002, but not PD98059 or U-73122, remarkably suppressed HB-EGF-induced migration of MLS cells (Figure 4B). These results confirmed that the HB-EGF-EGFR-PI3K/Akt axis was the dominant pathway involved in the HB-EGF-induced motility of MLS cells.

**Macrophage infiltration is a prognostic factor in MLS.** Finally, we investigated in detail the prognostic significance of macrophage infiltration into MLS. Univariate and multivariate analyses were performed using the following variables: number of CD68 cells, age, sex, location, tumour size, and round cell component (Table 1). Phosphorylated EGFR, metastasis, and AJCC stage were excluded because of their strong association with the number of CD68 cells. In univariate analysis, the number of CD68 cells and sex were significantly associated with poor prognosis. Multivariate analysis revealed that only the number of CD68 cells was an independent and significant factor for poor prognosis.

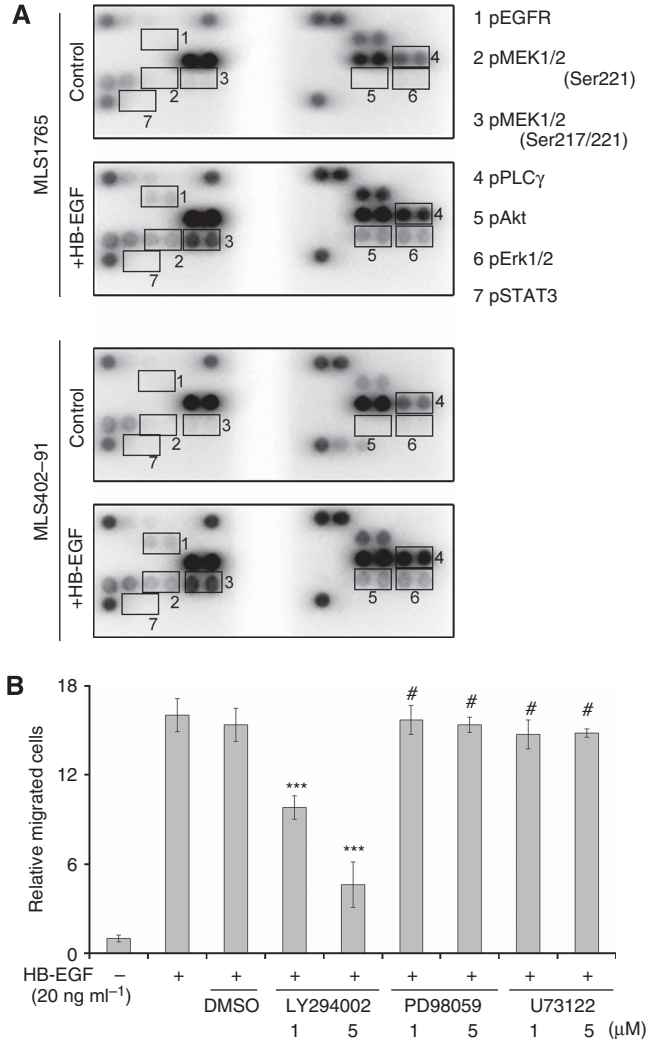


**Figure 4. The PI3K/Akt pathway was a key downstream signalling pathway in HB-EGF-induced motility of MLS cells.** (**A**) Analysis of EGFR-stimulated intracellular signalling modules using PathScan EGFR Signalling Antibody Array system. MLS1765 and MLS402-91 cell lysates either treated or not treated with HB-EGF (20 ng ml$^{-1}$) for 5 min were assessed. Each antibody was spotted in duplicate. (**B**) The effects of each inhibitor on HB-EGF-induced motility of MLS1765 cells were assessed using a Traswell migration assay with HB-EGF (20 ng ml$^{-1}$). HB-EGF was added to the lower chambers and each inhibitor was added to upper and lower chambers at the same time. Data are shown as mean ± s.d. ***$P<0.001$, #not significant.

## DISCUSSION

Metastasis occurs in up to one-third of MLS cases, and causes unfavourable outcomes. Tumour-associated macrophages have important roles in tumour invasion and metastasis (Condeelis and Pollard, 2006), and infiltration of TAMs into tumours results in tumour progression and poor prognosis. The presence of a high number of TAM is associated with various types of tumours, including bone and soft tissue tumours (Komohara *et al*, 2013). We previously reported that higher TAM infiltration was associated with poor prognosis in Ewing sarcoma (Fujiwara *et al*, 2011). In this study, we showed that greater TAM infiltration was associated with poor prognosis in MLS (Figure 1B), and its prognostic importance was confirmed in multivariate analysis (Table 1). On the basis of these results, TAMs are potentially a new prognostic factor for MLS. To our knowledge, this is the first report demonstrating an association between poor MLS prognosis and the role of TAMs.

In order for metastasis to occur, tumour cells must invade the extracellular matrix to separate from the primary lesion, intravasate to circulate towards distant organs, and then extravasate and engraft. In this study, we showed that macrophages promoted cell motility and invasion of MLS cells (Figure 2A–C). Furthermore, greater TAM infiltration was significantly correlated with the presence of metastasis (Supplementary Table S3). These results suggest that TAMs may have an important role in invasion and metastasis of MLS, especially during the first step involving dispatch from the primary lesion and intravasation. On the contrary, roles of TAMs in the later stages in MLS metastasis, such as during extravasation and homing to target organs, remain obscure. Thus further investigation, including *in vivo* experiments, is required.

It will be beneficial and interesting to define the mechanisms involved in TAM-induced motility and invasion of MLS cells. One possible mechanism is activation of the RTK pathway in MLS, since various RTKs, such as MET, IGF-1R, PDGFR, and EGFR, have been identified in MLS (Cheng *et al*, 2009; Negri *et al*, 2010). In MLS cells in this study, only EGFR, and not MET, IGF-1R, or PDGFR, was phosphorylated by M-CM *in vitro* (Figure 2D). Importantly, greater TAM infiltration in MLS was associated with higher expression of pEGFR in clinical samples (Figure 2I). These results offer solid evidence that TAMs enhance invasion and metastasis of MLS by activating the EGFR signalling pathway.

Identifying the key factors involved in TAM-induced activation of EGFR in MLS is the next important task that should be undertaken. Heparin-binding EGF-like growth factor is a member of the EGF family of molecules, which has a role in wound healing, cardiac hypertrophy, and heart development and function (Nanba and Higashiyama, 2004). In cancer, HB-EGF can contribute to tumour aggressiveness, including tumour proliferation, invasion, and metastasis, and there is growing evidence of the association between HB-EGF expression and poor cancer prognosis (Miyamoto *et al*, 2006). High expression of HB-EGF has also been detected in some soft tissue sarcomas and it is significantly associated with poor overall survival (Hoffmann *et al*, 2009). Furthermore, recent reports have shown that HB-EGF secreted by macrophages is a key factor in tumour progression in breast cancer (Vlaicu *et al*, 2013) and colon cancer (Rigo *et al*, 2010). In this study, we showed that HB-EGF enhanced migration and invasion of MLS cells via strong activation of EGFR (Figure 3B–F). On the basis of our findings and those of previous reports, we propose that HB-EGF is an important factor in TAM-induced invasion, metastasis, and activation of the EGFR pathway. Of the EGFR-stimulated downstream signalling modules in MLS, HB-EGF activated MEK1/2, Erk1/2, Akt, and PLCγ, but not STAT3 (Figure 4A). In this study, we confirmed that PI3K/Akt was the key pathway in MLS (Figure 4B). This result corresponded the previous findings that activation of PI3K/Akt pathway is associated with tumour survival, invasion, and poor prognosis in a variety of tumours (Engelman, 2009). In MLS, Demicco *et al* (2012) demonstrated that activation of the PI3K/Akt pathway was significantly associated with round cell change. Thus, HB-EGF secreted by TAMs in MLS might be one of the critical factors in activating the PI3K/Akt pathway that drives round cell transformation of MLS cells, therefore resulting in poor prognosis. This notion is intriguing, however, we were not able to confirm the association between macrophage infiltration and the round cell component in this study. Therefore, further studies are required to better understand the role of TAMs during the progression from myxoid to round cells.

From the findings of this study, we consider TAMs and HB-EGF to be potential molecular targets for treatment of MLS. In particular, CRM197, a non-toxic mutant of diphtheria toxin and a specific inhibitor of HB-EGF, has shown anticancer efficacy in

**Table 1. Results of univariate and multivariate analyses for overall survival**

| | Univariate | | Multivariate | |
|---|---|---|---|---|
| **Variable** | **HR (95% CI)** | ***P*-value** | **HR (95% CI)** | ***P*-value** |
| **Age** | | | | |
| ⩽40 ($n=27$) | 1 | 0.6244 | 1 | 0.9066 |
| >40 ($n=51$) | 1.32 (0.45–4.79) | | 1.08 (0.26–3.85) | |
| **Sex** | | | | |
| Male ($n=46$) | 4.95 (1.37–31.58) | 0.0114* | 3.43 (0.45–72.83) | 0.2527 |
| Female ($n=32$) | 1 | | 1 | |
| **Location** | | | | |
| Extremity ($n=63$) | 1 | 0.6322 | 1 | 0.0565 |
| Others ($n=14$) | 1.34 (0.35–4.06) | | 5.19 (0.95–25.80) | |
| **Tumour size** | | | | |
| ⩽5 cm ($n=14$) | 1 | 0.2528 | 1 | 0.4118 |
| >5 cm ($n=57$) | 2.83 (0.54–52.14) | | 2.41 (0.33–48.83) | |
| **Round cell component** | | | | |
| ⩽5% ($n=63$) | 1 | 0.1801 | 1 | 0.577 |
| >5% ($n=15$) | 2.07 (0.69–5.63) | | 1.51 (0.34–6.68) | |
| **CD68 numbers** | | | | |
| Low (<100/10 HPF) ($n=63$) | 1 | 0.0002*** | 1 | 0.0011** |
| High (⩾100/10 HPF) ($n=15$) | 7.00 (2.57–20.73) | | 8.11 (2.28–33.85) | |

Abbreviations: CI = confidence interval; HPF = high power field; HR = hazard ratio. *$P<0.05$, **$P<0.01$, ***$P<0.001$.

ovarian cancer both *in vitro* and *in vivo*, and clinical trials are now underway. Because this study confirmed the expression of HB-EGF in clinical samples of MLS as well as the biological effects of HB-EGF on malignant phenotypes of MLS cells (Figure 3), MLS could be a promising candidate for anti-HB-EGF agents.

In conclusion, the present study showed that macrophage infiltration predicted poor prognosis in MLS, and a possible underlying mechanism is that HB-EGF secretion by macrophages enhanced MLS cell motility and invasion by activating EGFR. The HB-EGF-EGFR-PI3K/Akt downstream signalling pathways had a dominant role in TAM-induced cell motility and invasion of MLS. Tumour-associated macrophages, HB-EGF, EGFR, and PI3K/Akt could be new candidates for therapeutic targets of MLS and thus further investigation is warranted.

## ACKNOWLEDGEMENTS

We thank Dr Junji Kishimoto for helpful suggestions on statistics. This work was supported by a Grant-in-Aid for Scientific Research (23592192, 25293325, and 26713046) from the Japan Society for the Promotion of Science, and a Grant-in-Aid for Clinical Research Evidence-Based Medicine and Cancer Research from the Ministry of Health, Labour and Welfare of Japan (Y Iwamoto).

## CONFLICT OF INTEREST

The authors declare no conflict of interest.

## REFERENCES

Aman P, Ron D, Mandahl N, Fioretos T, Heim S, Arheden K, Willen H, Rydholm A, Mitelman F (1992) Rearrangement of the transcription factor gene CHOP in myxoid liposarcomas with t(12;16)(q13;p11). *Genes Chromosomes Cancer* **5**(4): 278–285.

Antonescu CR, Ladanyi M (2013) Myxoid liposarcoma. In *World Health Organization Classification of Tumours: Pathology and Genetics of Tumours of Soft Tissue and Bone*, Fletcher CD, Bridge JA, Hogendoorn PC, Mertens F (eds)pp 39–41. IARC Press: Lyon.

Antonescu CR, Tschernyavsky SJ, Decuseara R, Leung DH, Woodruff JM, Brennan MF, Bridge JA, Neff JR, Goldblum JR, Ladanyi M (2001) Prognostic impact of P53 status, TLS-CHOP fusion transcript structure, and histological grade in myxoid liposarcoma: a molecular and clinicopathologic study of 82 cases. *Clin Cancer Res* **7**(12): 3977–3987.

Asano N, Susa M, Hosaka S, Nakayama R, Kobayashi E, Takeuchi K, Horiuchi K, Suzuki Y, Anazawa U, Mukai M, Toyama Y, Yabe H, Morioka H (2012) Metastatic patterns of myxoid/round cell liposarcoma: a review of a 25-year experience. *Sarcoma* **2012**: 345161.

Baay M, Brouwer A, Pauwels P, Peeters M, Lardon F (2011) Tumor cells and tumor-associated macrophages: secreted proteins as potential targets for therapy. *Clin Dev Immunol* **2011**: 565187.

Buddingh EP, Kuijjer ML, Duim RA, Burger H, Agelopoulos K, Myklebost O, Serra M, Mertens F, Hogendoorn PC, Lankester AC, Cleton-Jansen AM (2011) Tumor-infiltrating macrophages are associated with metastasis suppression in high-grade osteosarcoma: a rationale for treatment with macrophage activating agents. *Clin Cancer Res* **17**(8): 2110–2119.

Carr MW, Roth SJ, Luther E, Rose SS, Springer TA (1994) Monocyte chemoattractant protein 1 acts as a T-lymphocyte chemoattractant. *Proc Natl Acad Sci USA* **91**(9): 3652–3656.

Cheng H, Dodge J, Mehl E, Liu S, Poulin N, van de Rijn M, Nielsen TO (2009) Validation of immature adipogenic status and identification of prognostic biomarkers in myxoid liposarcoma using tissue microarrays. *Hum Pathol* **40**(9): 1244–1251.

Condeelis J, Pollard JW (2006) Macrophages: obligate partners for tumor cell migration, invasion, and metastasis. *Cell* **124**(2): 263–266.

Demicco EG, Torres KE, Ghadimi MP, Colombo C, Bolshakov S, Hoffman A, Peng T, Bovee JV, Wang WL, Lev D, Lazar AJ (2012) Involvement of the PI3K/Akt pathway in myxoid/round cell liposarcoma. *Mod Pathol* **25**(2): 212–221.

Engelman JA (2009) Targeting PI3K signalling in cancer: opportunities, challenges and limitations. *Nat Rev Cancer* **9**(8): 550–562.

Fujiwara-Okada Y, Matsumoto Y, Fukushi J, Setsu N, Matsuura S, Kamura S, Fujiwara T, Iida K, Hatano M, Nabeshima A, Yamada H, Ono M, Oda Y, Iwamoto Y (2013) Y-box binding protein-1 regulates cell proliferation and is associated with clinical outcomes of osteosarcoma. *Br J Cancer* **108**(4): 836–847.

Fujiwara T, Fukushi J, Yamamoto S, Matsumoto Y, Setsu N, Oda Y, Yamada H, Okada S, Watari K, Ono M, Kuwano M, Kamura S, Iida K, Okada Y, Koga M, Iwamoto Y (2011) Macrophage infiltration predicts a poor prognosis for human ewing sarcoma. *Am J Pathol* **179**(3): 1157–1170.

Goerdt S, Orfanos CE (1999) Other functions, other genes: alternative activation of antigen-presenting cells. *Immunity* **10**(2): 137–142.

Haniball J, Sumathi VP, Kindblom LG, Abudu A, Carter SR, Tillman RM, Jeys L, Spooner D, Peake D, Grimer RJ (2011) Prognostic factors and metastatic patterns in primary myxoid/round-cell liposarcoma. *Sarcoma* **2011**: 538085.

Harimaya K, Tanaka K, Matsumoto Y, Sato H, Matsuda S, Iwamoto Y (2000) Antioxidants inhibit TNFalpha-induced motility and invasion of human osteosarcoma cells: possible involvement of NFkappaB activation. *Clin Exp Metastasis* **18**(2): 121–129.

Hoffmann AC, Danenberg KD, Taubert H, Danenberg PV, Wuerl P (2009) A three-gene signature for outcome in soft tissue sarcoma. *Clin Cancer Res* **15**(16): 5191–5198.

Hubbard SR, Miller WT (2007) Receptor tyrosine kinases: mechanisms of activation and signaling. *Curr Opin Cell Biol* **19**(2): 117–123.

Iida K, Fukushi J, Matsumoto Y, Oda Y, Takahashi Y, Fujiwara T, Fujiwara-Okada Y, Hatano M, Nabashima A, Kamura S, Iwamoto Y (2013) miR-125b develops chemoresistance in Ewing sarcoma/primitive neuroectodermal tumor. *Cancer Cell Int* **13**(1): 21.

Kamura S, Matsumoto Y, Fukushi JI, Fujiwara T, Iida K, Okada Y, Iwamoto Y (2010) Basic fibroblast growth factor in the bone microenvironment enhances cell motility and invasion of Ewing's sarcoma family of tumours by activating the FGFR1-PI3K-Rac1 pathway. *Br J Cancer* **103**(3): 370–381.

Komohara Y, Jinushi M, Takeya M (2013) Clinical significance of macrophage heterogeneity in human malignant tumors. *Cancer Sci* **105**(1): 1–8.

Lee CH, Espinosa I, Vrijaldenhoven S, Subramanian S, Montgomery KD, Zhu S, Marinelli RJ, Peterse JL, Poulin N, Nielsen TO, West RB, Gilks CB, van de Rijn M (2008) Prognostic significance of macrophage infiltration in leiomyosarcomas. *Clin Cancer Res* **14**(5): 1423–1430.

Leek RD, Lewis CE, Whitehouse R, Greenall M, Clarke J, Harris AL (1996) Association of macrophage infiltration with angiogenesis and prognosis in invasive breast carcinoma. *Cancer Res* **56**(20): 4625–4629.

Matsumoto Y, Tanaka K, Hirata G, Hanada M, Matsuda S, Shuto T, Iwamoto Y (2002) Possible involvement of the vascular endothelial growth factor-Flt-1-focal adhesion kinase pathway in chemotaxis and the cell proliferation of osteoclast precursor cells in arthritic joints. *J Immunol* **168**(11): 5824–5831.

Miyamoto S, Yagi H, Yotsumoto F, Kawarabayashi T, Mekada E (2006) Heparin-binding epidermal growth factor-like growth factor as a novel targeting molecule for cancer therapy. *Cancer Sci* **97**(5): 341–347.

Nanba D, Higashiyama S (2004) Dual intracellular signaling by proteolytic cleavage of membrane-anchored heparin-binding EGF-like growth factor. *Cytokine Growth Factor Rev* **15**(1): 13–19.

Negri T, Virdis E, Brich S, Bozzi F, Tamborini E, Tarantino E, Jocolle G, Cassinelli G, Grosso F, Sanfilippo R, Casalini P, Greco A, Pierotti MA, Pilotti S (2010) Functional mapping of receptor tyrosine kinases in myxoid liposarcoma. *Clin Cancer Res* **16**(14): 3581–3593.

Oda Y, Yamamoto H, Takahira T, Kobayashi C, Kawaguchi K, Tateishi N, Nozuka Y, Tamiya S, Tanaka K, Matsuda S, Yokoyama R, Iwamoto Y, Tsuneyoshi M (2005) Frequent alteration of p16(INK4a)/p14(ARF) and p53 pathways in the round cell component of myxoid/round cell liposarcoma: p53 gene alterations and reduced p14(ARF) expression both correlate with poor prognosis. *J Pathol* **207**(4): 410–421.

Pietras K, Ostman A (2010) Hallmarks of cancer: interactions with the tumor stroma. *Exp Cell Res* **316**(8): 1324–1331.

Qian BZ, Pollard JW (2010) Macrophage diversity enhances tumor progression and metastasis. *Cell* **141**(1): 39–51.

Rigo A, Gottardi M, Zamo A, Mauri P, Bonifacio M, Krampera M, Damiani E, Pizzolo G, Vinante F (2010) Macrophages may promote cancer growth via a GM-CSF/HB-EGF paracrine loop that is enhanced by CXCL12. *Mol Cancer* **9**: 273.

Vlaicu P, Mertins P, Mayr T, Widschwendter P, Ataseven B, Hogel B, Eiermann W, Knyazev P, Ullrich A (2013) Monocytes/macrophages support mammary tumor invasivity by co-secreting lineage-specific EGFR ligands and a STAT3 activator. *BMC Cancer* **13**: 197.



Supplementary Information accompanies this paper on British Journal of Cancer website (http://www.nature.com/bjc)